Journal of Techniques, ISSN: 2708-8383, Vol. 6, No. 2, 2024, Pages 71-82
DOI: https://doi.org/10.51173/jt.v6i2.1915

JOURNAL OF TECHNIQUES

Journal homepage: http://journal.mtu.edu.iq

RESEARCH ARTICLE – ENGINEERING (MISCELLANEOUS)

Methodology for Using Multi-Temporal Landsat Images to Monitor Urban Growth of Kirkuk Governorate

Tabark Y. Gehad[1*], Nejat Q. Omer[2], Nada S. Abdulmajeed[1]

[1]Surveying Engineering Department, Technical Engineering College of Kirkuk, Northern Technical Kirkuk University, Kirkuk, Iraq

[2]Civil Engineering Department, University of Kirkuk, Kirkuk, Iraq

[*] Corresponding author E-mail: tabarak.yousef@ntu.edu.iq

Article Info.

Article history:

Received
24 August 2023

Accepted
20 October 2023

Published
30 June 2024

Abstract

The growth of cities around the world creates difficulties for governments due to the strain it puts on resources and the negative impact on the environment and living conditions for residents. The Kirkuk Governorate has experienced significant urban growth in recent years, causing various environmental, economic, and social issues. The study aims to monitor the growth of Kirkuk Governorate from 1990 to 2020 using multi-spectral Landsat images to better understand urban development. Landsat-5 TM for 1990, Landsat-7 ETM+ for 2000, Landsat-5 TM for 2010, and Landsat-8 OLI for 2020 were used for this study. The Supervised Maximum Likelihood algorithm was utilized to categorize images into urban and non-urban areas, with accuracy rates ranging from 91.25% to 96.66% between 1990 and 2020. Post-classification change detection analysis was also conducted to observe changes in urban growth, revealing that the studied city expanded from 46.96 km^2 to 193.25 km^2 over 30 years. Over the past thirty years, the urban area of Kirkuk Governorate has increased while the non-urban area has decreased. This increase is due to factors such as population growth, political changes, and economic development. This study provides valuable information about this urban growth and can be used as a foundation for future studies on the region's socioeconomic and environmental changes.

Publisher: Middle Technical University

Keywords: Urban Growth; Landsat; GIS; Kirkuk; Change Detection.

1. Introduction

The growth and expansion of urban areas around the world suggest that the future of the earth is predominantly urban, especially in less developed countries. This highlights the dynamic nature of these regions [1]. In the last 200 years, cities have become the most important places where people live all around the world. By 2050, 68% of the world's population will live in cities, which is called urbanization. However, this will mean that another 2.5 billion people will live in cities by 2050, and most of this growth will happen in Asia and Africa [2]. Urbanization refers to the transformation of rural land into urban areas, which is caused by various factors such as migration, economic growth, population increase, natural growth, improved social infrastructure, and availability of facilities and services [3-6]. Urban growth leads to urbanization, industrialization, and land development, but these developments have adverse impacts on the environment, traffic, and population [7]. The complex factors affecting urban land have consequences for its development and economic activity, both in the past, present, and future. Urbanization and its expansion have altered land use and coverage concerning climate change [8-10], the loss of forests and agricultural lands destroying plant and animal biodiversity [11], noise, air and water pollution, thereby affecting the quality of life [12] , changing the hydrological ecosystem [13-17]. However, changes in land use and cover have detrimental effects on natural resources and the socio-economic system, both directly and indirectly [18, 19].

In developing countries like Iraq, urbanization is a significant issue, with most community expansion occurring without proper planning. This means that the preparation of designs and plans for communities often falls behind population growth and urbanization [20]. The Kirkuk Governorate has experienced significant growth in recent years, largely due to the discovery of oil in the province in 1927. This led to economic and social changes that attracted people from other provinces, as well as political conflict, wars, and economic sanctions [21]. Fast urban growth and development lead to various issues, such as unplanned environmental pollution and the consumption of large agricultural and vacant lands. Therefore, sustainable development is necessary that includes providing all necessary facilities and monitoring to maintain the equilibrium within urban areas [22, 23]. Urban growth monitoring is the practice of using remote sensing data to track changes in urban areas over time.

One of the most crucial skills of remote sensing is the ability to monitor changes after the pictures have been adjusted [24]. Remote sensing refers to the monitoring of Earth's resources without touching them by using reflected or emitted electromagnetic energy [25]. Remote sensing technology provides various tools and techniques to monitor and measure the growth of urban areas and changes in land use through satellite

Nomenclature & Symbols			
GIS	Geographic Information System	USGS	United States Geological Survey
ETM+	Enhanced Thematic Mapper Plus	MLC	Maximum Likelihood Classification
LULC	Land Use/Land Cover	UTM	Universal Transverse Mercator
TM	Thematic Mapper	OLI/TIRS	Operational Land Imager and Thermal Infrared Sensor

data collected at different times and locations [26-28]. In this study, remote sensing refers to the collection of land surface information through Landsat imagery. Physical monitoring methods, on the other hand, are costly, time-consuming, tedious, and error-prone [29, 30]. Multispectral and multi-temporal remote sensing satellite imagery is a cost-effective and rapid way to assess the effects of human activities on Earth's land resources [31, 32] and can also provide statistically valid information on the spatial extent of cities [33, 34].

Remote sensing data, specifically moderate-resolution Landsat images, offer a suitable option for monitoring land use and land cover changes in developing countries where geospatial technologies are not well established [35, 36]. Due to their capacity to offer consistent coverage, a holistic view, instant data collection, and precise and economical details on transformations in land use and land cover [37, 38], The use of Landsat images and GIS technology is a common method for monitoring urban growth and its impact on ecosystems. GIS is a computer system that captures, stores, analyzes, and presents geographic data and has become an important tool for determining the direction of urban development [39, 40]. The flexible framework provided by GIS makes it possible to gather, store, display, and analyze the digital data required for change detection [41]. As a result, they have been widely used to create accurate urban development maps that can be used in urban planning and governance in several studies [42-45]. These studies show that using Landsat imagery is useful for tracking urban development by identifying changes in land cover and creating maps of it.

To accurately assess these changes, it is necessary to classify the satellite images. This classification process is crucial in digital image analysis and involves creating separate categories of land cover, also known as themes [25]. The most popular methods for classifying satellite images are supervised classification and unsupervised classification. Furthermore, unsupervised LULC classification techniques include fuzzy C-means clustering, K-means clustering, ISODATA (Iterative Self-Organizing Data Analysis), self-organizing maps, and neural networks, unsupervised classifiers such as ISODATA automatically classify satellite imagery into a user-defined number of groups based on similar spectral characteristics [46]. Unsupervised classifiers are useful when there is no prior knowledge available, but combining similar land use and land cover classes can be difficult and lead to lower accuracy. On the other hand, supervised classification methods like MLC, K-Nearest Neighbor, Support Vector Machines, and Random Forest Classifiers are beneficial [47]. However, supervised techniques can extrapolate or extend the available land cover data from known image sectors to classify unknown image sectors [48]. It is more controlled by the user than unsupervised classification. The LULC classifier that is most frequently used is MLC because it provides excellent accuracy by using land cover signatures that the user supplies [49-53]. Managing and regulating the expansion of cities in line with national urban development plans is a top priority in modern urban planning [54]. One useful method for tracking changes in the urban environment is the change detection technique. This technique allows for quantitative analysis of changes in the distribution of various categories within a given region. Increases or decreases in any category can be measured simultaneously [30]. This study aims to use remote sensing techniques to examine how urban and non-urban areas in the Kirkuk governorate have changed between 1990 and 2020. It also seeks to create a geographic database that includes spatial and descriptive information layers to assist decision-makers and planners in understanding the development and expansion of the governorate.

2. Materials and Methods

2.1. Study area

One of Iraq's historic areas, Kirkuk is home to a variety of ethnic groups and is known for its vibrant culture and illustrious past. It has a roughly 5,000-year history and occupies a key geographic spot between central and northern Iraq [21] which is located about 250 kilometers north of the country's capital (Baghdad). With a mean elevation of 350 m, it is located between latitudes 35° 23' and 35° 32' and longitudes 44° 26' and 44° 18'. Its approximate area is 9,745 km^2, making up 2.2 percent of all of Iraq's land. Kirkuk, Haweeja, Daquq, and Dibis are the four districts that make up the governorate of Kirkuk, as shown in Fig. 1. It covers a large area, has a wide range of natural features, and has had multilingual inhabitants for hundreds of years. Kirkuk experiences warm, semi-arid weather that is both much hotter and drier in the summer and cooler and more humid in the winter [55], Along with diverse economic resources, this city is described as having a diverse religious and ethnic population. It features substantial oil and gas reserves, which are regarded as one of Iraq's main financial resources. Additionally, it is made up of a variety of geographical regions, including plateaus, mountains, lowlands, and plains. Kirkuk serves as a prime example of productive land. Arable land, multiple irrigation projects, and fertile ground [56].

2.2. Data source

The study's objective can be easily accomplished with the aid of the technology offered by the various Landsat satellites. Since the launch of the first Landsat satellite in 1972, the program has played a significant role in supplying useful data for environmental monitoring, natural resource management, and worldwide change study because of the medium spatial resolution and the availability of long-term data [46], [55], Landsat is jointly managed by the United States Geological Survey (USGS) and NASA. The land sat satellites make a complete round of the world every 16 days, taking pictures as they fly overhead, covering the whole surface.

The study used four satellite images: Landsat- 5 Thermic Mapper sensor (TM), Landsat-7 Enhanced Thematic Mapper Plus (ETM+), and Landsat- 8 Operational Land Imager and Thermal Infrared Sensor (OLI/TIRS) as shown in Table 1. taken ten years apart from each other for thirty years between 1990 and 2020 they were obtained freely in Geotiff format with 30m-resolution from the USGS Earth Explorer https://earthexplorer.usgs.gov/ The USGS archive contains satellite images dated to 1972 and onwards of the entire world. To purchase imagery from the USGS, I had to create an account on their website to place an order for a download. All of the Landsat images utilized in this study are geo-referenced to the Universal Transverse Mercator (UTM) projection system (zone 38N, World Geodetic System 84). The relationship between the amount of cloud cover on satellite images and the quality of the classification of images is inverse. As a result, all images have been selected in the summer season with clouds covering less than 10% and free of haze contamination.

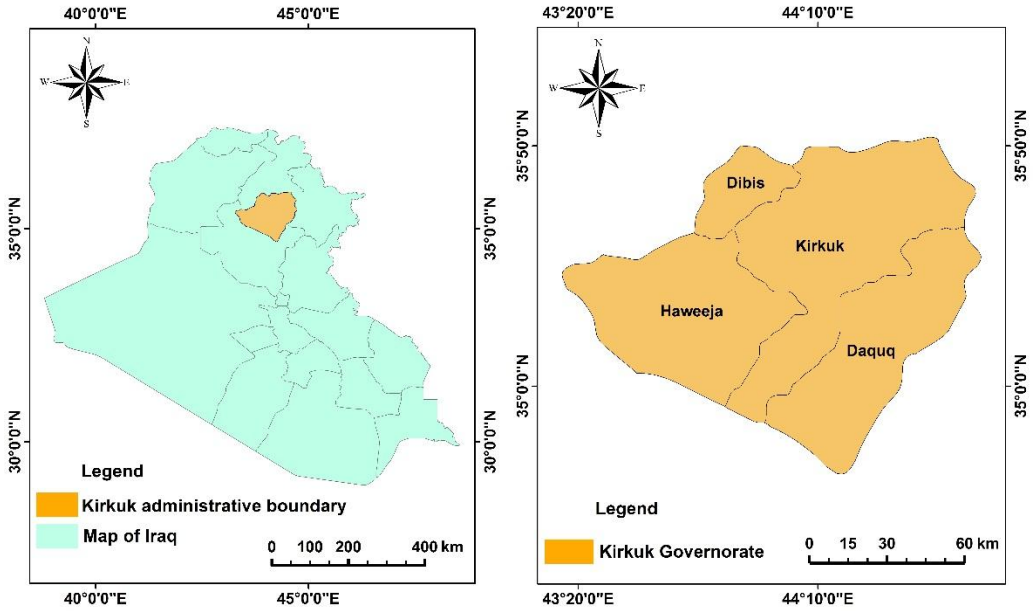

Fig. 1. Kirkuk Governorate, case study

Table 1. Landsat satellite images used in the study

Satellite	Sensor	Year	Resolution(M)	Acquisition Date	Path/Row
landsat5	TM	1990	30	1990/08/19	35/36
landsat7	ETM+	2000	30	2000/08/22	35/36
landsat5	TM	2010	30	2010/07/09	35/36
landsat8	OLI/TIRS	2020	30	2020/07/20	35/36

Source: USGS GLOVIS

2.3. Ancillary data

The relationship between population and urban growth is a fundamental aspect of modern society; in addition to the multispectral and multi-temporal images mentioned above, Population data of Kirkuk Governorate are used to view and compare changes over time, as shown in Table 2 from the Iraqi Ministry of Planning, Central Statistical Organization [57]. The growth rate was extracted using the population growth equation (Eq.1) [58] :

$$R = \sqrt[\tau]{\frac{P1}{P0}} - 1 \times 100 \quad (1)$$

R: population growth rate, *P*1: The population in the next census, *Po*: The population at the previous census, *T*: The number of years between the two censuses

Table 2. The population of Kirkuk Governorate and growth rate between (1997-2020)

Year	No. of population	Rate of growth
1997	753171	2.3%
2009	1325853	4.8%
2020	1682809	2.2%

Table 2 provides data on the rate of population growth, the number of people, and the corresponding years for three specific points in time: 1997, 2009, and 2020.

2.4. Methodology

The suggested methodology is divided into several major stages, as shown in Fig. 2.

2.4.1. Preprocessing images

It is a fundamental step that is necessary for preparing raw data for more advanced procedures [59]. The Landsat images have been processed and analyzed with ArcGIS 10.3. The USGS Level-1 data is provided as individual band images in the Georeferenced Tagged Image File Format (also known as Geo TIFF). To work with these images, all the individual band images should be combined into a single image. All bands are combined using ArcGIS 10.3, excluding the thermal band due to its coarse resolution. To obtain the overall LULC information for the study area, bands 3, 2, and 1 of Landsat TM were combined to generate false-color images. For Landsat ETM+ images, bands 5, 4, and 3 were combined. For Landsat OLI/TIRS images, bands 7, 6, and 4 were combined, which improved the visual interpretation and increased the spectral separation to distinguish the urban class from other land cover classes. Then, two images were acquired and mosaicked for each of the years of the study to cover the whole study area, which was clipped using a common shapefile.

2.4.2. Image classification

Supervised classification is a common image-processing method for identifying changes in land surface features in various multi-spectral global datasets [60]. It is more accurate than other classification methods. In supervised classification, software used to analyze images is trained to identify pixels with similar spectral features [61]. To observe and quantify urban growth, the maximum likelihood supervised classification (MLC) method in ARC GIS 10.3 was employed for classifying the Landsat images because of its simplicity and robustness, which predict pixel probability for the highest likelihood based on Bayes' theorem [62, 63]. Based on the statistical characteristics of the training samples for each class developed by the user, the algorithm determines the likelihood that a pixel belongs to each class. The pixel is then given the class with the highest probability.

For each of the preprocessed images, a minimum of 150 training samples were collected—75 samples for each land cover category—by using the Landsat Image and interpreting historical aerial images in Google Earth. Then, the software generates spectral signatures for each class based on the supplied information. Next, the images are classified by applying the Maximum Likelihood algorithm. The (MLC) assigns pixels that have the highest probability of belonging to that class. Two major classes of Landsat images were classified (urban areas and non-urban areas) according to the USGS scheme of Anderson's plan [64]. All different kinds of built-up and non-built-up areas were combined, as shown in Table 3. The Anderson schema is a flexible hierarchy system that can be used at multiple levels depending on the level of detail and scope required by the application.

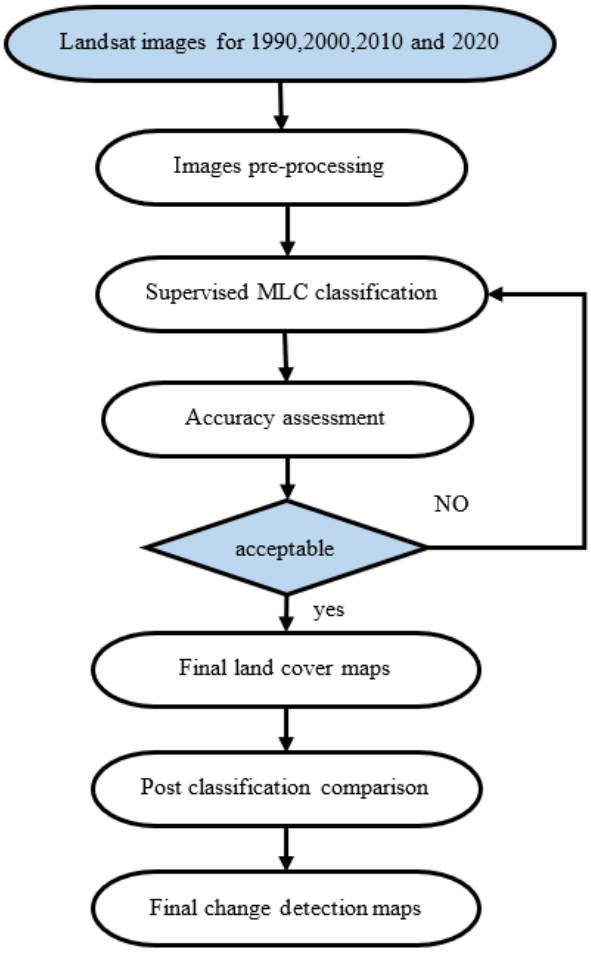

Fig. 2. The overall workflow for this study

Table 3. Description of LULC classes

Class	Description
urban areas	(Residential, commercial and services, industrial, transportation, communication, and utilities)
non-urban areas	(bar land, water bodies, mountains, vegetation, agricultural land)

2.4.3. Accuracy assessment

Sample points were selected (reference data) randomly researched in the ArcMap from different locations, accurately calculated by high-resolution images from Google Earth archives. Overall accuracy is the total number of corrected samples divided by the total number of samples and converted to a percentage. The producer's accuracy is determined by dividing the total number of pixels obtained from reference data by the number of accurate pixels in one class. The user's accuracy is calculated by dividing the total number of sets recognized in a class by the number of sets that were correctly identified in that class. The Kappa coefficient is one of the most popular measures for resolving discrepancies between the actual agreement and the chance agreement [65]. Kappa values ranging from 0.61 to 1.00 are considered to be good to excellent [66]. The Kappa statistics are computed by the following (Eq. 2).

$$K = \frac{N \sum_{i=1}^{r} x_{ii} - \sum_{i=1}^{r} (x_{i+} \times x_{+i})}{N^2 - \sum_{i=1}^{r} (x_{i+} \times x_{+i})} \quad (2)$$

where K is the Kappa coefficient, N is the total number of observations, r is the number of rows and columns in the error matrix, xii is the number of observations in row i and column I, xi+ and x+i are the marginal totals of row i and column i, respectively [67].

2.4.4. Land cover change detection

The variation in land cover between the 1990–2000, 2000–2010, and 2010–2020 periods was determined by the difference in the values of 1990, 2000, 2010, and 2020 of the same class [68], which are shown in Equations (3).

Temporal LC change = (Area final year - area initial year)/ (area initial year) ×100 (3)

In this study post classification change matrix determines the change in land cover from classified images of 1900 to 2000, 2000 to 2010, and 2010 to 2020. This is a very popular quantitative change detection algorithm used to create maps of land cover change by comparing two or more independently classified images from different dates.

3. Result and Discussion

3.1. Classification accuracy assessment

Accuracy assessment plays a crucial role in remote sensing analysis for land use and land cover classification. In this study, the overall accuracy was evaluated using an error matrix employing the stratified random sample method. Table 4 presents an accurate assessment of land cover classes for the years 1990, 2000, 2010, and 2020.

Table 4. Accuracy assessment of land cover classes for 1990, 2000, 2010, and 2020

Land Cover	1990		2000		2010		2020	
	User Accuracy	Producer Accuracy	User Accuracy	Producer Accuracy	User Accuracy	ProducerAccuray	User Accuracy	ProducerAccuray
urban	96.15	80.64	93.61	86.27	100	80.51	95.94	95.94
Non-urban	88.88	97.95	93.26	97	86.23	100	97.16	97.16
Overall accuracy (%)	91.25		93.37		91.22		96.66	
Kappa coefficient	0.81		0.84		0.81		0.93	

Table 4 demonstrates that the accuracy of land cover classification has generally improved over the years, with high user and producer accuracies for both Urban and Non-urban classes. The results indicated that the overall accuracy percentages were 91% in 1990, 93% in 2000, 91% in 2010, and 96% in 2020. Additionally, the overall kappa statistics were found to be 0.81 in 1990, 0.84 in 2000, 0.81 in 2010, and 0.93 in 2020, indicating substantial agreement between the map classifications and the actual land cover on the ground. The high overall accuracy and Kappa coefficients suggest that the classification method used is reliable and has become more accurate over time, especially in the classification of land cover for the year 2020.

3.2. Classification results

The study area's land cover (LC) was divided into urban and non-urban categories. To accomplish this classification, the maximum supervised classification technique was applied using GIS techniques. The resulting classified images for the years 1990, 2000, 2010, and 2020 are presented in Fig. 3, respectively. These images serve as valuable resources for analyzing the land cover changes within the research area. Using GIS functionality to extract classes from each cover map, Table 5 shows the area in km^2 of land cover classes; the urban area covered 46.96km^2 (0.48%) in 1990 and increased to 59.49km^2 (0.61%) in 2000; these areas increased further to113.08km^2 (1.16%) by the year 2010 and 193.25km^2 (1.98%) in 2020. The urban area grew by (146.29) km^2 during the period 1990-2020. Non-urban areas, on the other hand, have decreased substantially from 9698.31km^2 (99.51%) in 1900 to a mere 9685.80km^2 (99.38%) in the year 2000. These areas decreased further to 9632.2km^2 (98.83%) by the year 2010 and 9551.84km^2 (98.01%) in 2020, a record loss of 146.47 km^2 in the 30 years of the study period. Temporal changes in the areas are shown in Fig. 4.

Table 5. Area of land cover classes each year

	1990		2000		2010		2020	
Area	km^2	%	km^2	%	km^2	%	km^2	%
Urban	46.96	0.48	59.49	0.61	113.08	1.16	193.25	1.98
Non-urban	9698.31	99.51	9685.80	99.38	9632.2	98.83	9551.84	98.01

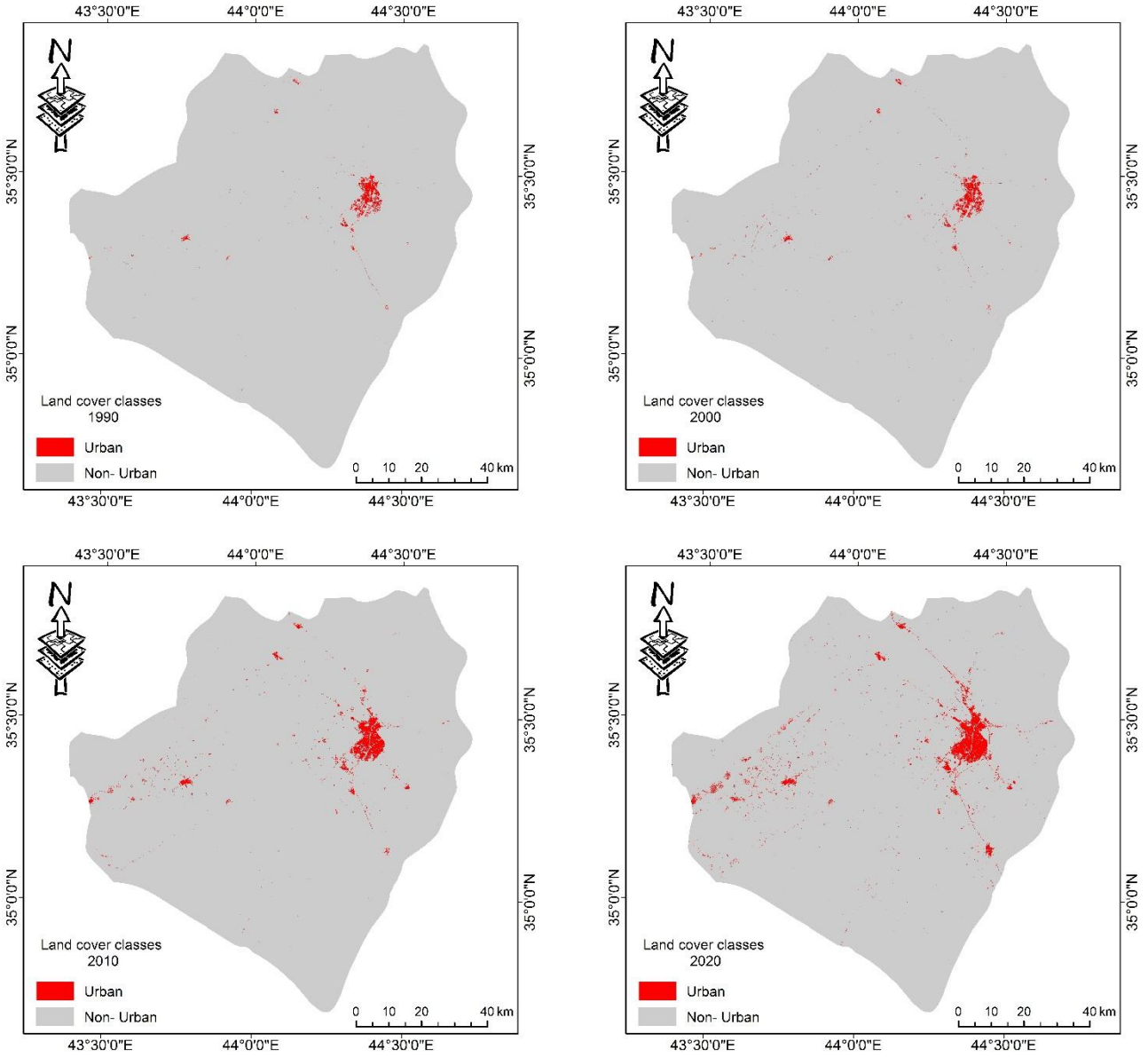

Fig. 3. Land cover classes of the study area in 1990, 2000, 2010, and 2020

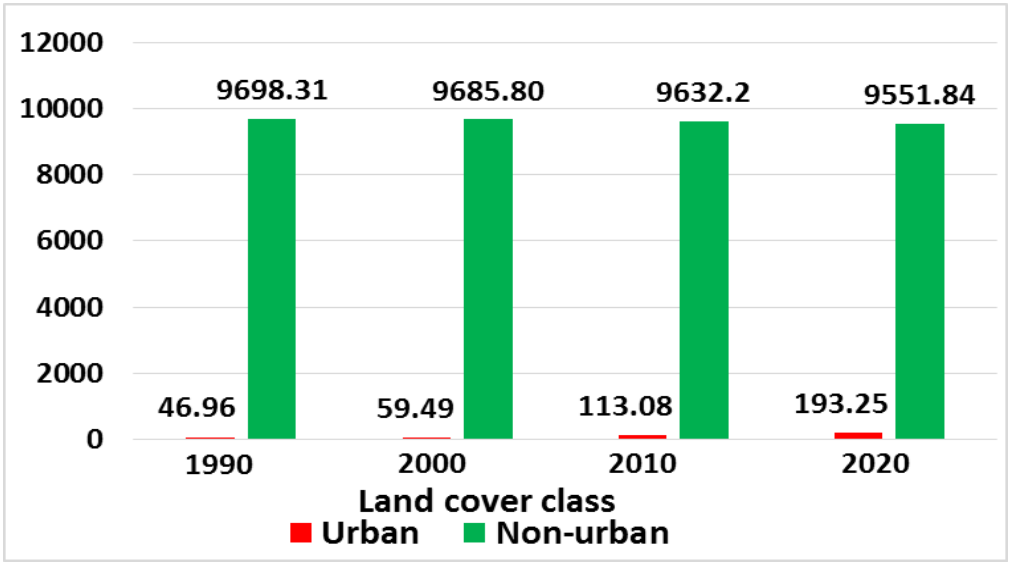

Fig. 4. Temporal change of land cover classes during the four periods

3.3. Land cover change dynamics from1990 to 2020

The temporal rate of change (Table 6) was utilized to analyze the land cover change in each LC (Land Cover) class and enable a comparison among the different classes across the three periods. This approach provides valuable information regarding the rate of change for each specific land cover class over time.

Table 6. Rate of change in land cover classes over time

LC	Rate of change%		
	2000-1990	2010-2000	2020-2010
urban	26.68	90	70.89
non-urban	-0.13	-0.55	-0.83

In 1990, there were 46.96 km^2 (0.48%) of urban area, this number raised to 59.49 km^2 (0.61%) in 2000, in 2010 the urban area covered 113.08 km^2(1.16%) of the total area and 193.25 km^2 (1.98%) in 2020. According to this, a 26.68% temporal increase was observed over 10 years, from 1990 to 2000, a 90% temporal increase was seen from 2000 to 2010, and a 70.89% temporal increase was seen from 2010 to 2020. In 1990, the non-urban area covered 9698.31 km^2(99.51%), which fell to 9685.8 km^2 (99.38 %) in 2000. In 2010, the non-urban area covered 9632.2 km^2 (98.83%) and 9551.84 km^2 (98.01%). This showed that between 1990 and 2000, a 0.13% temporal decline was realized; 0.55% temporal reductions were observed between 2000 and 2010, and a 0.83% temporal decline was observed between 2010 and 2020.

The post-classification comparison approach was employed for detection of land cover changes from 1990 to 2000, 2000 to 2010 and 2010 to 2020, by comparing independently produced classified land cover maps. The main advantage of this method is its capability to provide descriptive information on the nature of changes that occurs. Figs. 5, 6, and 7 show the change detection maps. Meanwhile, Tables 7, 8, and 9 provide detailed statistics regarding the transition of land cover (LC) classes.

According to Table 7, analyzing land cover changes between 1990 and 2000, there was a notable growth in the urban area, amounting to 59.47 km^2. However, a portion of this expansion was converted into non-urban areas, totaling 8.45 km^2 because of the government's policy at that time, many of the people of Kirkuk were displaced. During the same period, there was a decrease in the non-urban area of 12.51 km^2, indicating a shrinkage. Interestingly, a portion of this non-urban area was transformed into urban areas, expanding by 20.97 km^2.

During the 2000-2010 period, a comparable pattern to that of 1990-2000 was observed. The urban area experienced an increase of 53.59 km^2, while simultaneously a portion of its area was converted into non-urban areas, amounting to 8.76 km^2 due to the volatile political events including, the 2003 war. The non-urban areas continued to decrease, reaching 9632.19 km^2, with 62.35 km^2 of them being transformed into urban areas, as indicated in Table 8.

Between 2010 and 2020, the urban area witnessed significant growth, expanding to 193.24 km^2. However, during this period, a portion of 14.81 km^2 was converted into non-urban areas because of the Iraqi civil war in 2014; the once thriving urban space has undergone a profound transformation, lost its characteristic features, and became a non-urban environment. In contrast, the non-urban area encompassed 9630.18 km^2 in 2010, but by 2020, it decreased to 9,550.01 km^2. Approximately 94.98 km^2 of this reduction were converted into urban areas, as indicated in Table 9.

This research provides a comprehensive overview of urban growth in Kirkuk, encompassing valuable information regarding the spatial distribution and magnitude of urban expansion. Over the study period, the urban area exhibited a general increase in all directions, with particular emphasis on expansion along highways, primarily in regions equipped with essential services for the city's residents. The study area, along with Iraq as a whole, has faced challenging circumstances that have significantly affected its urban growth. These difficulties were primarily shaped by volatile political events, including the economic blockade, the 2003 war, and the second Iraqi civil war in 2014. As a result, the once thriving urban area has undergone a profound transformation, lost its characteristic features, and become a non-urban area. Kirkuk governorate is regarded as a commercial hub in the northern region due to its exceptional geographic location that links the northern and southern governorates. In particular, following the nationalization of oil in the province in 1972 and the subsequent improvement in economic and living conditions, the region gained significant prominence. This attracted people from all governorates of life, particularly those seeking employment opportunities in oil and gas companies, resulting in a notable population surge. The region has experienced exponential growth in population due to the rising number of natural population and the successive migration from other provinces. The population of the governorate was recorded as 753,171 people in 1997. Over time, the city's population continued to increase, and by 2009, it had reached 1,325,853 individuals, with a growth rate of 4.8%. By the year 2020, the population of Kirkuk Governorate had grown to 1,682,809 individuals, with a growth rate of 2.2%. The significant population growth in the Kirkuk area has caused the observed changes in land cover depicted in the change detection maps. This influx has led to rapid urbanization and has affected the morphology of the city. As a result, the urban area has expanded alongside the increase in population. The expansion of urban areas, whether legal or illegal, has significant consequences on agricultural lands and other land uses, resulting in adverse impacts on the environment, economy, and society Consequently, the study emphasizes the urgent need for ongoing monitoring of urban growth trends. To curb the horizontal expansion of urbanization at the expense of agricultural lands, the promotion of vertical building extension for residential purposes is advocated, aiming to reduce the land area utilized for construction to preserve essential farmland for future generations.

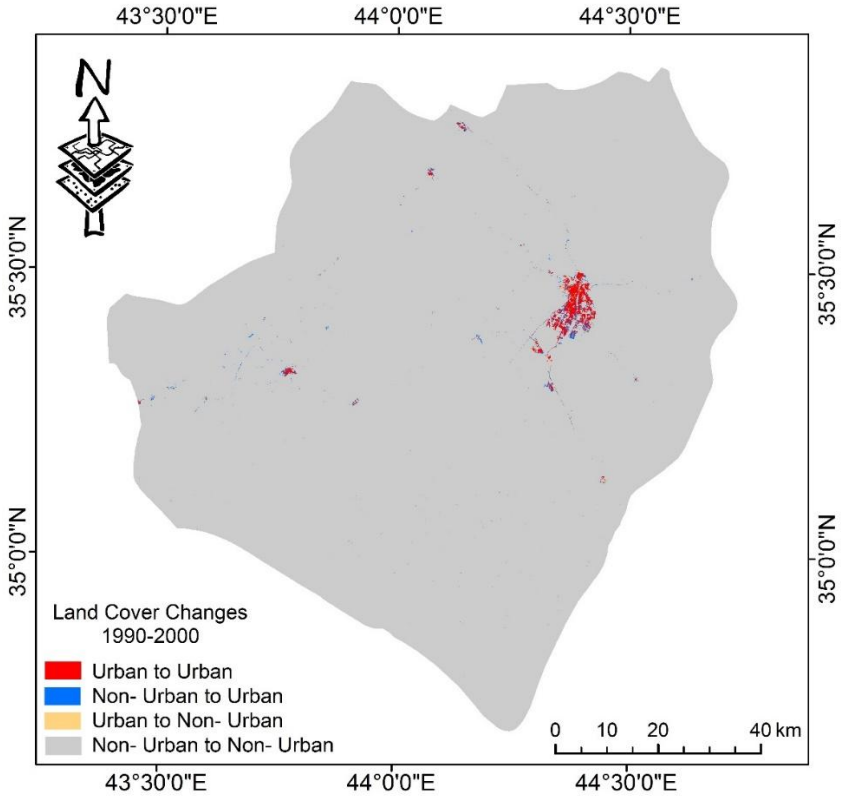

Fig. 5. Land cover change between 1990-2000

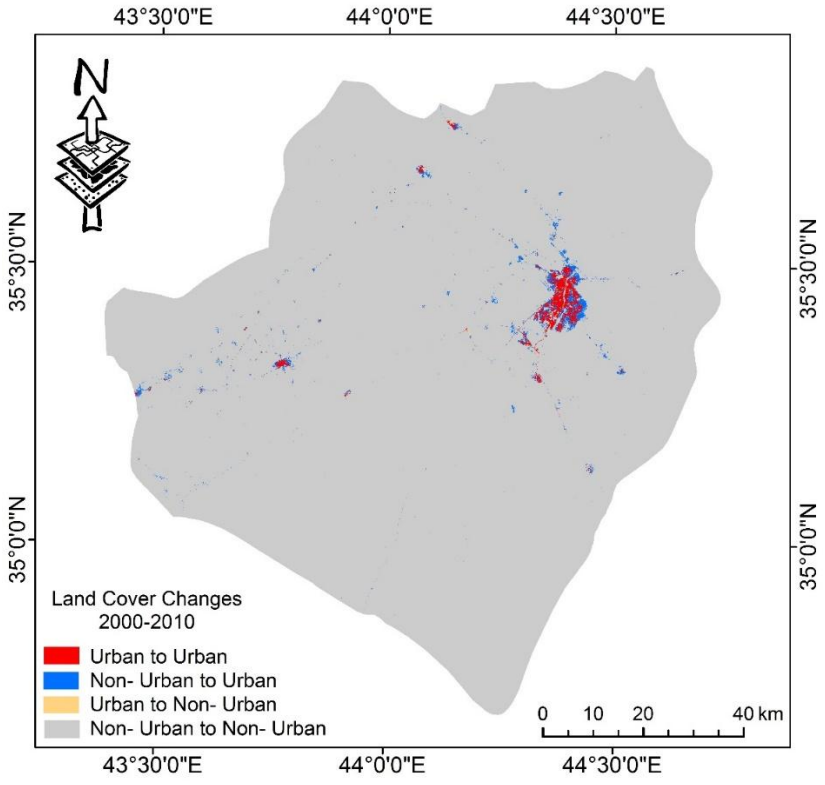

Fig. 6. Land cover change between 2000-2010

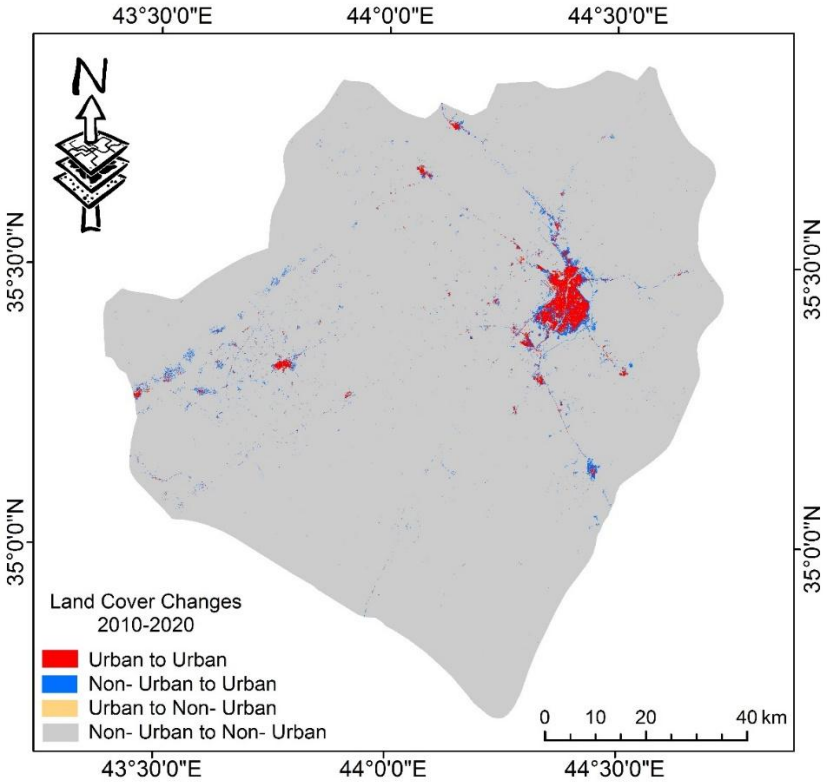

Fig 7. Land cover change between 2010-2020

Table 7. Land cover change statistics (1990-2000)

		change to LC 2000 (km^2)		
	LC	**urban km^2**	**non-urban km^2**	**Total**
change from LC1990 (km^2)	Urban	38.5	8.45	46.95
	non-urban	20.97	9677.22	9698.19
	Total	59.47	9685.67	

Table 8. Land cover change statistics (2000-2010)

		change to LC 2010 (km^2)		
	LC	**urban km^2**	**non-urban km^2**	**Total**
change from LC2000(km^2)	urban	50.72	8.76	59.48
	non-urban	62.35	9623.43	9685.78
	total	113.07	9632.19	

Table 9. Land cover change statistics (2010-2020)

		change to LC 2020 (km^2)		
	LC	**urban km^2**	**non-urban km^2**	**Total**
change from LC2010 (km^2)	Urban	98.26	14.81	113.07
	non-urban	94.98	9535.2	9630.18
	total	193.24	9550.01	

4. Conclusion

In this research study, a quantitative analysis was performed to examine the urban growth in Kirkuk governorate spanning from 1990 to 2020. The study employed readily accessible Landsat images with a resolution of 30m x 30m, along with maximum likelihood algorithms and a Post-Classification Change Matrix in conjunction with GIS, to effectively map and monitor changes in land cover. To ensure the accuracy of the findings, an assessment was conducted on the classified images, which contributed to the provision of more reliable information concerning the growth of the governorate. The research outcomes indicate that the combination of GIS technology and remote sensing holds substantial value as a robust and indispensable tool in such studies.

From 1990 to 2020, the urban conurbation of Kirkuk experienced significant growth both in size and density. The urban area expanded from 46.96 km^2 in 1990 to 193.25 km^2 in 2020, indicating a substantial increase. The main catalyst behind this rapid urban growth is the continuously growing population of Kirkuk. Given the ongoing population increase and the government's dedication to meeting the demand for residential, commercial, and industrial lands, it is expected that urban expansion will persist in the near future. The availability of detailed spatial and temporal data on historical urban growth plays a crucial role in enhancing our understanding of the dynamics of growth. By providing reliable long-term urban land cover maps spanning several decades, it becomes possible to investigate the current factors driving urban growth in the city and comprehend the resulting consequences. Moreover, such data assists in predicting the future trajectory of the city under various

socioeconomic and environmental scenarios, bringing benefits to scientists, government institutions, private sectors, landowners, and policymakers alike. They gain valuable insights into the outcomes of extensive urban growth and can establish policies and measures that promote the sustainability of the city.

Acknowledgment

The authors wish to express their gratitude for the collaboration and support provided by Engineering Technical College/Kirkuk, which greatly contributed to the completion of this research.

References

[1] P. Shehu, L. S. Rikko, and M. B. Azi, "Monitoring urban growth and changes in land use and land cover: a strategy for sustainable urban development," Int. J. Hum. Cap. Urban Manag., vol. 8, no. 1, pp. 111–126, 2023. DOI: 10.22034/IJHCUM.2023.01.09.
[2] United Nations, "Revision of World Urbanization Prospects.," 2018. https://www.un.org/development/desa/en/news/population/2018-revision-of-world-urbanization-prospects.html.
[3] R. B. Bhagat and S. Mohanty, "Emerging pattern of urbanization and the contribution of migration in urban growth in India," Asian Popul. Stud., vol. 5, no. 1, pp. 5–20, 2009. https://doi.org/10.1080/17441730902790024.
[4] B. Bhatta, Analysis of urban growth and sprawl from remote sensing data. Springer Science & Business Media, 2010. DOI: 10.1007/978-3-642-05299-6.
[5] L. Altieri, D. Cocchi, G. Pezzi, E. M. Scott, and M. Ventrucci, "Urban sprawl scatterplots for Urban Morphological Zones data," Ecol. Indic., vol. 36, pp. 315–323, 2014. https://doi.org/10.1016/j.ecolind.2013.07.011.
[6] S. Das and D. P. Angadi, "Land use land cover change detection and monitoring of urban growth using remote sensing and GIS techniques: A micro-level study," GeoJournal, vol. 87, no. 3, pp. 2101–2123, 2022. https://doi.org/10.1007/s40808-018-0547-5.
[7] T. A. Akbar, Q. K. Hassan, S. Ishaq, M. Batool, H. J. Butt, and H. Jabbar, "Investigative spatial distribution and modelling of existing and future urban land changes and its impact on urbanization and economy," Remote Sens., vol. 11, no. 2, p. 105, 2019. https://doi.org/10.3390/rs11020105.
[8] M. Acheampong, Q. Yu, L. D. Enomah, J. Anchang, and M. Eduful, "Land use/cover change in Ghana's oil city: Assessing the impact of neoliberal economic policies and implications for sustainable development goal number one–A remote sensing and GIS approach," Land use policy, vol. 73, pp. 373–384, 2018. https://doi.org/10.1016/j.landusepol.2018.02.019.
[9] H. H. Nguyen, F. Recknagel, and W. Meyer, "Effects of projected urbanization and climate change on flow and nutrient loads of a Mediterranean catchment in South Australia," Ecohydrol. Hydrobiol., vol. 19, no. 2, pp. 279–288, 2019. https://doi.org/10.1016/j.ecohyd.2018.10.001.
[10] S. M. Oswald et al., "Using urban climate modelling and improved land use classifications to support climate change adaptation in urban environments: A case study for the city of Klagenfurt, Austria," Urban Clim., vol. 31, p. 100582, 2020. https://doi.org/10.1016/j.uclim.2020.100582.
[11] S. Mansour, M. Al-Belushi, and T. Al-Awadhi, "Monitoring land use and land cover changes in the mountainous cities of Oman using GIS and CA-Markov modelling techniques," Land use policy, vol. 91, p. 104414, 2020. https://doi.org/10.1016/j.landusepol.2019.104414.
[12] S. Chaturvedi, K. Shukla, E. Rajasekar, and N. Bhatt, "A spatio-temporal assessment and prediction of Ahmedabad's urban growth between 1990–2030," J. Geogr. Sci., vol. 32, no. 9, pp. 1791–1812, 2022. https://doi.org/10.1016/j.ejrs.2019.05.001
[13] D. Maktav and F. S. Erbek, "Analysis of urban growth using multi-temporal satellite data in Istanbul, Turkey," Int. J. Remote Sens., vol. 26, no. 4, pp. 797–810, 2005. https://doi.org/10.1080/01431160512331316784.
[14] B. R. Pickard, D. Van Berkel, A. Petrasova, and R. K. Meentemeyer, "Forecasts of urbanization scenarios reveal trade-offs between landscape change and ecosystem services," Landsc. Ecol., vol. 32, pp. 617–634, 2017. DOI 10.1007/s10980-016-0465-8.
[15] S. Patra, S. Sahoo, P. Mishra, and S. C. Mahapatra, "Impacts of urbanization on land use/cover changes and its probable implications on local climate and groundwater level," J. urban Manag., vol. 7, no. 2, pp. 70–84, 2018. https://doi.org/10.1016/j.jum.2018.04.006.
[16] J. Kim and J. H. Ryu, "Modeling hydrological and environmental consequences of climate change and urbanization in the Boise River Watershed, Idaho," JAWRA J. Am. Water Resour. Assoc., vol. 55, no. 1, pp. 133–153, 2019. https://doi.org/10.3390/w12092436.
[17] I. Dutta and A. Das, "Application of geo-spatial indices for detection of growth dynamics and forms of expansion in English Bazar Urban Agglomeration, West Bengal," J. Urban Manag., vol. 8, no. 2, pp. 288–302, 2019. https://doi.org/10.1016/j.jum.2019.03.007.
[18] M. M. Katyambo and M. M. Ngigi, "Spatial monitoring of urban growth using GIS and remote sensing: a case study of Nairobi metropolitan area, Kenya," 2017, DOI: 10.5923/j.ajgis.20170602.03.
[19] S. Rahaman, P. Kumar, R. Chen, M. E. Meadows, and R. B. Singh, "Remote sensing assessment of the impact of land use and land cover change on the environment of Barddhaman district, West Bengal, India," Front. Environ. Sci., vol. 8, p. 127, 2020. https://doi.org/10.3389/fenvs.2020.00127.
[20] N. H. Hamed, M. M. Bayati, and H. R. Mohammed, "Digital Change Detection and Map Analysis for Urban Expansion and Land Cover Changes in Karbala City," Eng. Technol. J., vol. 38, no. 9, pp. 1246–1256, 2020. https://doi.org/10.30684/etj.v38i9A.296.
[21] N. Q. Omar, S. A. M. Sanusi, W. M. W. Hussin, N. Samat, and K. S. Mohammed, "Markov-CA model using analytical hierarchy process and multiregression technique," in IOP conference series: earth and environmental science, 2014, vol. 20, no. 1, p. 12008. DOI 10.1088/1755-1315/20/1/012008.
[22] J. A. Vinoth Kumar, S. K. Pathan, and R. J. Bhanderi, "Spatio-temporal analysis for monitoring urban growth–a case study of Indore city," J. Indian Soc. Remote Sens., vol. 35, pp. 11–20, 2007. doi:10.1007/bf02991829.
[23] T. Mugiraneza, S. Hafner, J. Haas, and Y. Ban, "Monitoring urbanization and environmental impact in Kigali, Rwanda using Sentinel-2 MSI data and ecosystem service bundles," Int. J. Appl. Earth Obs. Geoinf., vol. 109, p. 102775, 2022. https://doi.org/10.1016/j.jag.2022.102775.
[24] U. Choudhury and R. Kanga, "Gis And Stochastic Based Assessment And Modelling Of Urban Growth Patterns - A Review,", Suresh Gyan Vihar University journal of climate change and water, vol. 9, pp. 27–45, 2022.
[25] T. Lillesand, R. W. Kiefer, and J. Chipman, Remote sensing and image interpretation. John Wiley & Sons, 2015.

[26] R. Sharma, A. Ghosh, and P. K. Joshi, "Analysing spatio-temporal footprints of urbanization on environment of Surat city using satellite-derived bio-physical parameters," Geocarto Int., vol. 28, no. 5, pp. 420–438, 2013. https://doi.org/10.1080/10106049.2012.715208.
[27] D. Dutta, A. Rahman, and A. Kundu, "Growth of Dehradun city: An application of linear spectral unmixing (LSU) technique using multi-temporal landsat satellite data sets," Remote Sens. Appl. Soc. Environ., vol. 1, pp. 98–111, 2015. https://doi.org/10.1016/j.rsase.2015.07.001.
[28] L. H. Nguyen, S. V Nghiem, and G. M. Henebry, "Expansion of major urban areas in the US Great Plains from 2000 to 2009 using satellite scatterometer data," Remote Sens. Environ., vol. 204, pp. 524–533, 2018. https://doi.org/10.1016/j.rse.2017.10.004.
[29] C. R. Suribabu, J. Bhaskar, and T. R. Neelakantan, "Land use/cover change detection of Tiruchirapalli City, India, using integrated remote sensing and GIS tools," J. Indian Soc. Remote Sens., vol. 40, pp. 699–708, 2012. DOI 10.1007/s12524-011-0196-x.
[30] S. Singh and K. Sarma, "Analyzing the change in land cover dynamics: A case study of Delhi," 2023. https://doi.org/10.21203/rs.3.rs-2743780/v1.
[31] V. N. Mishra and P. K. Rai, "A remote sensing aided multi-layer perceptron-Markov chain analysis for land use and land cover change prediction in Patna district (Bihar), India," Arab. J. Geosci., vol. 9, pp. 1–18, 2016. DOI 10.1007/s12517-015-2138-3.
[32] F. Ahmad, L. Goparaju, and A. Qayum, "LULC analysis of urban spaces using Markov chain predictive model at Ranchi in India," Spat. Inf. Res., vol. 25, no. 3, pp. 351–359, 2017. DOI 10.1007/s41324-017-0102-x.
[33] B. Rimal, L. Zhang, H. Keshtkar, B. N. Haack, S. Rijal, and P. Zhang, "Land use/land cover dynamics and modeling of urban land expansion by the integration of cellular automata and markov chain," ISPRS Int. J. Geo-Information, vol. 7, no. 4, p. 154, 2018. https://doi.org/10.3390/ijgi7040154
[34] F. Hossain and M. Moniruzzaman, "Environmental change detection through remote sensing technique: A study of Rohingya refugee camp area (Ukhia and Teknaf sub-district), Cox's Bazar, Bangladesh," Environ. Challenges, vol. 2, p. 100024, 2021. https://doi.org/10.1016/j.envc.2021.100024.
[35] M. O. Adepoju, A. C. Millington, and K. T. Tansey, "Land use/land cover change detection in metropolitan Lagos (Nigeria): 1984–2002," in ASPRS 2006 Annual Conference Reno, Nevada May, 2006, pp. 1–5.
[36] M. K. Leta, T. A. Demissie, and J. Tränckner, "Hydrological responses of watershed to historical and future land use land cover change dynamics of Nashe watershed, Ethiopia," Water, vol. 13, no. 17, p. 2372, 2021. https://doi.org/10.3390/w13172372.
[37] W. Pervaiz, V. Uddin, S. A. Khan, and J. A. Khan, "Satellite-based land use mapping: comparative analysis of Landsat-8, Advanced Land Imager, and big data Hyperion imagery," J. Appl. Remote Sens., vol. 10, no. 2, p. 26004, 2016. https://doi.org/10.1117/1.JRS.10.026004.
[38] A. Koranteng, I. Adu-Poku, E. Donkor, and T. Zawiła-Niedźwiecki, "Geospatial assessment of land use and land cover dynamics in the mid-zone of Ghana," Folia For. Pol. Ser. A. For., vol. 62, no. 4, pp. 288–305, 2020. http://dx.doi.org/10.2478/ffp-2020-0028
[39] M. M. Aburas, S. H. O. Abdullah, M. F. Ramli, and Z. H. Asha'ari, "Land suitability analysis of urban growth in Seremban Malaysia, using GIS based analytical hierarchy process," Procedia Eng., vol. 198, pp. 1128–1136, 2017. https://doi.org/10.1016/j.proeng.2017.07.155.
[40] S. I. Wadeea, R. M. Hamdoon, and M. S. Al-Zuhairy, "Effects of Industrial Wastewater on Water Quality Tigris River at Baghdad Using (GIS) Technique," J. Tech., vol. 4, no. 4, pp. 1–11, 2022, [Online]. Available: https://journal.mtu.edu.iq/index.php/MTU/article/view/569. doi.org/10.51173/jt.v4i4.569.
[41] S. Panwar and D. S. Malik, "Evaluating land use/land cover change dynamics in Bhimtal lake catchment area, using remote sensing & GIS techniques," J. Remote Sens. GIS, vol. 6, no. 199, p. 2, 2017. DOI: 10.4172/2469-4134.1000199.
[42] D. Aldogom, N. Aburaed, M. Al-Saad, S. Al Mansoori, M. R. Al Shamsi, and A. A. Al Maazmi, "Multi temporal satellite images for growth detection and urban sprawl analysis; Dubai City, UAE," in Remote Sensing Technologies and Applications in Urban Environments IV, 2019, vol. 11157, pp. 71–81. https://doi.org/10.1117/12.2533097.
[43] A. F. Koko, W. Yue, G. A. Abubakar, A. A. N. Alabsi, and R. Hamed, "Spatiotemporal influence of land use/land cover change dynamics on surface urban heat island: A case study of Abuja metropolis, Nigeria," ISPRS Int. J. Geo-Information, vol. 10, no. 5, p. 272, 2021. https://doi.org/10.3390/ijgi10050272.
[44] V. Chettry, "Revision of world urbanization prospects," Environ. Monit. Assess., vol. 194, no. 12, p. 860, 2022.
[45] R. W. Aslam, H. Shu, and A. Yaseen, "Monitoring the population change and urban growth of four major Pakistan cities through spatial analysis of open source data," Ann. GIS, pp. 1–13, 2023. https://doi.org/10.1080/19475683.2023.2166989.
[46] I. R. Hegazy and M. R. Kaloop, "Monitoring urban growth and land use change detection with GIS and remote sensing techniques in Daqahlia governorate Egypt," Int. J. Sustain. Built Environ., vol. 4, no. 1, pp. 117–124, 2015. https://doi.org/10.1016/j.ijsbe.2015.02.005.
[47] S. N. MohanRajan, A. Loganathan, and P. Manoharan, "Survey on Land Use/Land Cover (LU/LC) change analysis in remote sensing and GIS environment: Techniques and Challenges," Environ. Sci. Pollut. Res., vol. 27, pp. 29900–29926, 2020. https://doi.org/10.1007/s11356-020-09091-7.
[48] H. B. Wakode, K. Baier, R. Jha, and R. Azzam, "Analysis of urban growth using Landsat TM/ETM data and GIS—a case study of Hyderabad, India," Arab. J. Geosci., vol. 7, pp. 109–121, 2014. DOI 10.1007/s12517-013-0843-3.
[49] M. Usman, R. Liedl, M. A. Shahid, and A. Abbas, "Land use/land cover classification and its change detection using multi-temporal MODIS NDVI data," J. Geogr. Sci., vol. 25, pp. 1479–1506, 2015. N. T. I. Ismael, "Urban expansion indicators of cities "Case study for Arab cities," J. Tech., vol. 2, no. 1, pp. 1–21, 2020, doi: 10.51173/jt.v2i1.51.
[50] T. W. Meshesha, S. K. Tripathi, and D. Khare, "Analyses of land use and land cover change dynamics using GIS and remote sensing during 1984 and 2015 in the Beressa Watershed Northern Central Highland of Ethiopia," Model. Earth Syst. Environ., vol. 2, pp. 1–12, 2016. DOI 10.1007/s40808-016-0233-4.
[51] S. Kaliraj, N. Chandrasekar, K. K. Ramachandran, Y. Srinivas, and S. Saravanan, "Coastal landuse and land cover change and transformations of Kanyakumari coast, India using remote sensing and GIS," Egypt. J. Remote Sens. Sp. Sci., vol. 20, no. 2, pp. 169–185, 2017. https://doi.org/10.1016/j.ejrs.2017.04.003.
[52] S. Bagaeen and H. Hijazi, "The role of land use change in developing city spatial models in Jordan: The case of the Irbid master plan (1970–2017)," Alexandria Eng. J., vol. 58, no. 3, pp. 861–875, 2019. https://doi.org/10.1016/j.aej.2019.08.001.
[53] S. Chaturvedi, K. Shukla, E. Rajasekar, and N. Bhatt, "A spatio-temporal assessment and prediction of Ahmedabad's urban growth between 1990–2030," J. Geogr. Sci., vol. 32, no. 9, pp. 1791–1812, 2022, https://doi.org/10.1007/s11442-022-2023-4.
[54] N. T. I. Ismael, "Urban expansion indicators of cities "Case study for Arab cities," J. Tech., vol. 2, no. 1, pp. 1–21, 2020, doi: 10.51173/jt.v2i1.51.

[55] E. Belief, "GIS based spatial modeling to mapping and estimation relative risk of different diseases using inverse distance weighting (IDW) interpolation algorithm and evidential belief function (EBF)(Case study: Minor Part of Kirkuk City, Iraq)," Int J Eng Technol, vol. 7, no. 4.37, pp. 185–191, 2018, https://doi.org/10.14419/ijet.v7i4.37.24098.

[56] A. M. Noori, W. M. Qader, F. G. Saed, and Z. A. Hamdany, "Quantification of morphometric parameters to analyze the watershed characteristics: A case study of Rosti Watershed, Iraq," Int. J. Adv. Sci. Technol., vol. 28, no. 13, pp. 273–289, 2019.

[57] Central statistics Organisation, "Yearly Statistics Report (2020 Part Two).Ministry of Planning in Iraq," p. 42, 2020.

[58] W. B. F. John I. Clarke, W. B. Fisher, Population Geography (2nd ed.). Elsevier Science. Retrieved from. 2013. [Online]. Available: https://www.perlego.com/book/1897927/population-geography-pergamon-oxford-geographies-pdf (Original work published 2013).

[59] A. Asokan and J. Anitha, "Change detection techniques for remote sensing applications: A survey," Earth Sci. Informatics, vol. 12, pp. 143–160, 2019. doi:10.1007/s12145-019-00380-5. https://doi.org/10.1007/s12145-019-00380-5.

[60] M. K. Jat, P. K. Garg, and D. Khare, "Monitoring and modelling of urban sprawl using remote sensing and GIS techniques," Int. J. Appl. earth Obs. Geoinf., vol. 10, no. 1, pp. 26–43, 2008. https://doi.org/10.1016/j.jag.2007.04.002.

[61] M. T. Rahman, "Detection of land use/land cover changes and urban sprawl in Al-Khobar, Saudi Arabia: An analysis of multi-temporal remote sensing data," ISPRS Int. J. Geo-Information, vol. 5, no. 2, p. 15, 2016. https://doi.org/10.3390/ijgi5020015.

[62] K. Alkaradaghi, S. S. Ali, N. Al-Ansari, and J. Laue, "Land use classification and change detection using multi-temporal Landsat imagery in Sulaimaniyah Governorate, Iraq," in Advances in Remote Sensing and Geo Informatics Applications: Proceedings of the 1st Springer Conference of the Arabian Journal of Geosciences (CAJG-1), Tunisia 2018, 2019, pp. 117–120. https://doi.org/10.1007/978-3-030-01440-7_28.

[63] W. M. M. Al-Hameedi, J. Chen, C. Faichia, B. Nath, B. Al-Shaibah, and A. Al-Aizari, "Geospatial Analysis of Land Use/Cover Change and Land Surface Temperature for Landscape Risk Pattern Change Evaluation of Baghdad City, Iraq, Using CA–Markov and ANN Models," Sustainability, vol. 14, no. 14, p. 8568, 2022. https://doi.org/10.3390/su14148568.

[64] J. R. Anderson, A land use and land cover classification system for use with remote sensor data, vol. 964. US Government Printing Office, 1976.

[65] G. M. Foody, "Status of land cover classification accuracy assessment," Remote Sens. Environ., vol. 80, no. 1, pp. 185–201, 2002. https://doi.org/10.1016/S0034-4257(01)00295-4.

[66] M. L. McHugh, "Interrater reliability: the kappa statistic," Biochem. medica, vol. 22, no. 3, pp. 276–282, 2012.

[67] R. G. Congalton, R. G. Oderwald, and R. A. Mead, "Assessing Landsat classification accuracy using discrete multivariate analysis statistical techniques," Photogramm. Eng. Remote Sensing, vol. 49, no. 12, pp. 1671–1678, 1983.

[68] M. Mathewos, S. M. Lencha, and M. Tsegaye, "Land use and land cover change assessment and future predictions in the Matenchose Watershed, Rift Valley Basin, using CA-Markov simulation," Land, vol. 11, no. 10, p. 1632, 2022. https://doi.org/10.3390/land11101632.